Materials & Structures manuscript No.
(will be inserted by the editor)

Unusual water transport properties of some traditional Scottish shale bricks

Isobel M. Griffin · Christopher Hall · Andrea Hamilton

Received: date / Accepted: date

Abstract Sorptivity, porosity and pore size distribution have been measured for five types of pressed fired-clay bricks recovered from a Second World War airfield in East Lothian, Scotland. It was found that the bricks, all manufactured locally from colliery shale, had similar porosities but significantly different compositions, leading to differences in pore structure and transport properties. Unusually high concentrations of organic carbon were found by analysis. In imbibition tests using water and *n*-decane, capillary absorption generally did not scale with time$^{1/2}$, indicating material non-uniformity in the flow direction. A sharp front *n*-layer model was used to estimate the variation of sorptivity and permeability in drilled cores taken through bed and stretcher

Isobel M Griffin · Christopher Hall · Andrea Hamilton

School of Engineering, University of Edinburgh, Edinburgh EH9 3JL, United Kingdom

Tel.: +44 131 650 4860

E-mail: andrea.hamilton@ed.ac.uk

faces. A surface skin of lower sorptivity was found in some materials. This is attributed to compression of the green clay in the brick mould during manufacture. Comparison of water and decane imbibition showed that water sorptivity is reduced throughout by partial wettability. This hydrophobicity of these shale bricks is tentatively related to their high organic carbon content, which is incompletely burned out during firing. We show how the partial wettability may be expressed in terms of a wetting index derived from imbibition data.

Keywords fired-clay brick · sorptivity · water flow in heterogeneous materials

Fig. 1 A Prestongrange pressed brick showing the maker's stamp on the bed face (230 mm × 115 mm).

1 Introduction

Large quantities of fired-clay bricks were manufactured from colliery shale waste in southern central Scotland from the mid nineteenth century until the 1970s [1–5]. These bricks were used widely in both domestic and industrial building. Colliery shales produce a stiff raw material and bricks were invariably made by pressing rather than extrusion [6]. The bricks frequently carried a maker's stamp (Fig 1) [7]. The shale was often heavily contaminated with coal which was at least partially burned out during firing. It is common practice in Scottish vernacular construction to apply lime or cement renders to the external face of brick masonry so that the variable appearance of these shale bricks was of little consequence. Colliery shale bricks have been produced in several other countries (including USA, France and Germany), and there is now renewed interest in colliery brick manufacture for waste utilisation, notably in China [8] and Korea [9].

We report here results from a study of the sorptivity properties of a small group of such traditional shale bricks. This work forms part of an analysis of the moisture dynamics of a number of historic brick masonry buildings in need of conservation. Knowledge of the water transport properties of brick materials is confined largely to recent production materials tested at the time of manufacture. Much less is known about traditional materials and those which form the fabric of existing buildings. This paper may also be of wider scientific interest in dealing with capillary imbibition behaviour in extremely non-uniform materials.

2 Sorptivity

Realistic estimates of water transport properties are essential for moisture dynamics analysis of building elements and whole buildings. For many purposes, sharp front models of water transport are powerful and useful [10–14], and for these the sorptivity is the material property of paramount importance.

The sorptivity S is usually determined by tests in which the cumulative capillary absorption i is measured as a function of time t. S can then be estimated from the relation $i = St^{1/2}$. This works well for homogeneous materials, however the $t^{1/2}$ law of capillary absorption does not hold for materials which are coarsely non-uniform and heterogeneous in the direction of flow. Generally, without an $i(t)$ dataset that is linear in $t^{1/2}$ the sorptivity is considered to be undefined. However, considerable progress has been made in the analysis of water transport in composite materials [10], and we show here how $i(t)$ data from heterogeneous materials may be analysed to show the variation of local sorptivity within a porous material.

Fig. 2 A typical cement rendered brick masonry building at East Fortune airfield, East Lothian, Scotland. These buildings followed the standard designs produced during World War II by the Ministry of Defence, and were virtually identical to military buildings elsewhere in the UK [15,16]. The walls were built in stretcher bond, a half brick thick (about 120 mm), with brick piers at 3.3 m intervals, protruding both internally and externally.

3 Materials and methods

The bricks we describe were used in the construction of the cement rendered brick masonry buildings on the military airfield at East Fortune, East Lothian, Scotland (Fig 2). The part of the airfield dating from the World War II is open to the public as the Scottish National Museum of Flight. As the site is a Scheduled Ancient Historic Monument it is not possible to take large samples of the building fabric, but brick materials were obtained from rubble from dismantled buildings.

The five types of bricks taken for study were identified by makers' stamps (Fig 1) as from Edinburgh, Niddrie, Prestongrange, Wallyford, and Whitehill. The last four are the names of colliery brickworks within 20 miles or so of East Fortune. Bricks with an

Fig. 3 Drilled cores from the colliery-shale bricks. From left to right: Edinburgh, Niddrie, Prestongrange, Wallyford, and Whitehill. Grid 1 cm × 1 cm.

Edinburgh stamp were manufactured at Wallyford up to 1947. Four of the five types, Edinburgh, Niddrie, Prestongrange and Whitehill, are present in the standing WWII buildings on the site. The Wallyford brick has not been found in the standing buildings but is included as an example of another local shale brick. It is known to be at least 40 years old, the Wallyford brickworks having closed in the early 1970s [17]. All the bricks tested were solid (unperforated), with frogs.

The bricks were cut in half in a direction parallel to the header face, and cores approximately 25 mm in diameter and 45-80 mm long were taken by drilling into the stretcher and bed faces (Fig 3). The external and internal surfaces of the bricks were examined without magnification. Petrographic thin sections were prepared to show composition and pore structure, and examined at up to 200× magnification. Mineral composition was also established by powder X-ray diffraction (Bruker D8), and total

organic carbon content by combustion analysis (Carlo Erba NA2500 Elemental Analyser).

Porosity was measured using a vacuum saturation technique, and mercury intrusion pore-size distribution was also determined (Autopore IV 9500 V1.07). The MIP samples were mostly taken from the interior of the bricks, but a sample of the surface skin of the Prestongrange bricks was also tested.

Water transport properties were investigated by capillary absorption measurements on the drilled cores, using the gravimetric method widely used for sorptivity testing [19, 10]. In some cases, the cores were cut across the cylinder axis to form two parts so that absorption behaviour in flow both towards the surface and towards the centre of the brick could be measured. Water and the hydrocarbon *n*-decane were used as absorption liquids. By comparing water and *n*-decane we are able to see any effects caused by partial (incomplete) wetting [10]. Tests were carried out at a laboratory temperature of 21±1°C and we use the following values for physical quantities: *Water*, viscosity 0.890 mPa s, surface tension 72.0 mN/m, density 997.0 kg/m^3; *n*-decane, viscosity 0.838 mPa s, surface tension 23.4 mN/m, density 726 kg/m^3.

4 Composition, physical properties and microstructure

Fig 4 shows a Prestongrange brick cut parallel to the header face. The section shows a coarse texture, with large quartz grains, extensive fissuring (here parallel to the bed faces), and a grey/black heart, with paler rim. The appearance is typical of the five shale brick types.

As observed at low magnification, all bricks consist of uniformly coloured matrices with various inclusions, some measuring up to 5 mm. Each brick has its own distinctive

Fig. 4 Section through a Prestongrange brick (approximately 70 mm × 105 mm), viewed with the bed faces at the top and bottom, showing large horizontal cracks parallel to the bed face.

matrix colour and mix of inclusions: the Niddrie bricks have a mid-brown matrix with burnt and unburnt coal particles, some of which were highly porous. The Wallyford bricks have a dark brown matrix and contain shrunken fragments of mudstone. The Prestongrange bricks have a light brown matrix with purplish inclusions of fireclay, and purple areas of high porosity, perhaps fireclay inclusions that had not fully vitrified.

Mineral composition is given in Table 1. The mineralogy and crystallinity evident in the XRD patterns indicates that the firing temperature for all of the bricks was around 1000–1100 °C with a soaking time of at least 12 hours to account for the observed quantities of mullite and cristobalite [21]. For Prestongrange and Wallyford bricks, the soaking time may have been longer. The presence of cordierite [21], a rare constituent of bricks, which only forms at temperatures above 1050°C and requires a

Table 1 Composition of shale bricks. Mineral content is expressed semi-quantitatively in wt%

Brick type	Quartz	Mullite	Cristobalite	Cordierite	Hematite	TOC (interior/surface)
	–					ppt[a]
Edinburgh	54	24	12	2	2	4.4/1.0
Niddrie	49	36	10	1	4	0.5/4.3
Prestongrange	13	53	13	17	3	17/3.9
Wallyford	40	34	12	9	4	103/3.4
Whitehill	16	61	19	2	1	1.6/1.1

Notes:

a Parts per thousand

Calcite content was < 1 wt% in all bricks, except in one Edinburgh sample (7 wt%)

long soaking time, in excess of 50 hours [22]also needs magnesium to be available in the starting clay mix [21].

In this case magnesium is probably released during breakdown of the original smectite present in the shale inclusions, as noted by Dunham [21]. He found that cordierite was formed only from a single carboniferous shale in the twelve different clay formations he investigated. None of the colliery shale bricks presented here contain high temperature Ca-pyroxene phases (diopside), Ca-pyroxenoid (wollastonite) or Ca-feldspar (anorthite) or indeed any feldspars. In fact, the starting clay was Ca poor to have produced none of these phases at all. Calcite is clear in one sample of Edinburgh brick only and its formation must be secondary, probably through leaching of the applied lime render.

All bricks have notably high organic carbon contents (Table 1). These values should be compared to a value of about 0.3 ppt as measured in a modern production brick.

Table 2 Properties of shale bricks

Brick type	Volume-fraction porosity –	Pore size distribution[a] small capillaries	medium capillaries	large capillaries	small voids	large voids	Bulk density kg/m^3	Solid density kg/m^3
Edinburgh	0.262	0.008	0.024	0.141	0.066	0.023	1790	2430
Niddrie	0.245	0	0.002	0.174	0.047	0.024	1895	2510
Prestongrange								
interior	0.268	0.015	0.059	0.076	0.087	0.031	1735	2370
skin	0.210	0	0.021	0.059	0.082	0.048	–	–
Wallyford	0.254	0.006	0.039	0.075	0.102	0.032	1665	2230
Whitehill	0.274	0.003	0.016	0.101	0.139	0.015	1685	2320

Notes: *a* Capillary pores, small $< 0.01\,\mu$m; medium 0.01–0.05 μm; large 0.05–10 μm; voids small 10–50 μm; large $> 50\,\mu$m [18]

Estimated uncertainties: porosity ± 0.005; bulk density ± 20 kg/m^3; solid density ± 30 kg/m^3

The TOC is generally higher in the core than at the surface, indicating incomplete burn out during firing [20]. Wallyford brick shows an exceptionally high carbon content in the core.

The volume fraction porosity and the bulk density of all five brick types (Table 2) lie in the ranges 0.24–0.27 and 1665–1895 kg/m^3 respectively. When the porosity is plotted against the measured bulk density, these bricks lie well below the general trend line found previously [23, 6, 10] for UK clay brick and which corresponds to a solid density of about 2620 kg/m^3. The calculated solid density of these Scottish shale bricks (Table 2) is in the range 2230–2510 kg/m^3.

5 Imbibition analysis

The water imbibition behaviour is very variable from brick to brick despite their similar porosities. Capillary absorption i in Edinburgh and Prestongrange bricks does not scale with $t^{1/2}$. Given that other causes of non-linearity [24, 10] are absent, this behaviour is a strong indication of material non-uniformity in the flow direction. In Fig 5 we show results from tests on cores drilled normal to the stretcher face and to the bed face of an Edinburgh brick. It is immediately clear from the experimental data that there is a definite surface skin of lower sorptivity. As we see this in tests with n-decane (Fig 5A), we must conclude that the variation of properties arises in part at least from intrinsic variation in porosity and pore structure.

5.1 The n-layer model

Water transport through the bricks is fitted with the Sharp Front n-layer model [31, 10] which describes 1D capillary imbibition into a rectangular bar, composed of n layers of arbitrary thickness and stacked parallel to the inflow face.

We assume (as in all SF models) that the capillary flow is controlled by three material properties, the porosity f, the permeability K, and the capillary potential Ψ_f at the wet front. For a uniform material, all three quantities are constant throughout the system. For absorption into an initially dry uniform column through one inflow face the flow velocity $u = \mathrm{d}i/\mathrm{d}t = -fK\Psi_\mathrm{f}/i$ so that $i = (2fK|\Psi_\mathrm{f}|)^{1/2}t^{1/2}$, where i is the cumulative absorption (absorbed volume per unit area of inflow surface). Therefore we link the sorptivity with the quantity $(2fK|\Psi_\mathrm{f}|)^{1/2}$ and assume an effective porosity, which takes air trapping into account and is typically about 80 per cent of the

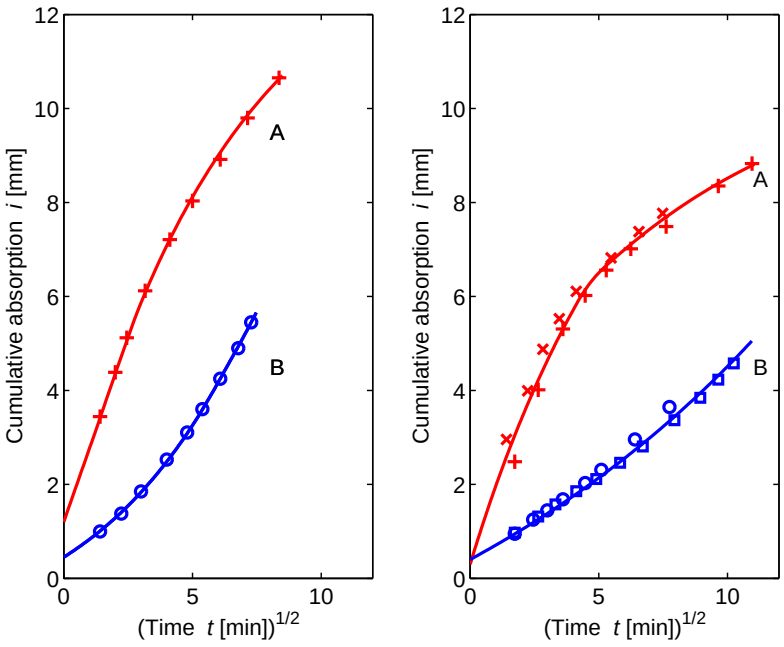

Fig. 5 Cumulative liquid absorption i vs $t^{1/2}$ in Edinburgh brick. Solid curves are fits to n-layer model with $n = 100$. *Left*: Imbibition of n-decane into a stretcher face core (length 60.8 mm × 24.4 mm diameter). *A*: Skin up, flow towards the surface skin; *B*: Skin down, flow towards the interior. *Right*: Imbibition of water into a bed face core (length 55.1 mm × 24.4 mm diameter). *A*: Skin up, flow towards the surface skin (repeat tests, +, ×); *B*: Skin down, flow towards the interior (repeat tests, ◯, □).

volume fraction open porosity. The permeability K is correspondingly the hydraulic conductivity of the wetted region at water content f.

In *non-uniform* materials, where the material properties f, K and $\Psi_{\rm f}$ may vary along the flow path, $t^{1/2}$ behaviour is not found [10]. A non-uniform 1-D system can

be represented by n layers (segments) of arbitrary thickness L_j and with different material properties, S_j, f_j and K_j. Then the cumulative absorption $i(t)$ is easily found by calculating the time t_{Jj} for the wet front to reach each of the $n-1$ junctions in turn, using a boot strapping algorithm [31]:

$$t_{Jj} = t_{J(j-1)} + \frac{f_j^2}{S_j^2} L_j^2 \left(1 + 2\frac{L_{e(j-1)}}{L_j}\right), \tag{1}$$

with $t_{J0} = 0$ and $L_{e0} = 0$, and where the equivalent length $L_{e(j-1)} = K_j \sum_{i=1}^{j-1} L_i/K_i$. The cumulative absorption at each t_J is then the sum of the fully wetted fluid contents of all preceding layers. Therefore

$$i(t_{Jj}) = \sum_{1}^{j} f_j L_j. \tag{2}$$

In a non-uniform system the quantities f, K, and Ψ_f are each well defined locally, so we assume that in a non-uniform material there is a variation in local sorptivity $S = (2fK|\Psi_\mathrm{f}|)^{1/2}$. This is a useful means of representing the nature of the non-uniformity and composites. However a knowledge of the sorptivity variation alone is insufficient, and we must know how all three quantities f, K and Ψ_f vary with position. In applying the n-layer analysis to a continuous variation of transport properties within materials such as brick, stone and concrete, it is possible that these quantities may be correlated rather than independent.

For liquids having dynamic viscosity η, surface tension σ and density ρ, the permeability $K \sim \rho/\eta$. For complete wetting, the capillary potential $\Psi_\mathrm{f} \sim \sigma/\rho$. Therefore, the sorptivity $S = (2fK|\Psi_\mathrm{f}|)^{1/2} \sim (\sigma/\eta)^{1/2}$. Similarly, by applying these scalings to Eqn 1, we see that the times $t_{Jj} \sim \sigma/\eta$.

We find that the observed $i(t)$ data are well represented by the n-layer model [31, 10]. Using a large value of n (generally 100), we discretise a continuous variation of

properties along the core. Since liquid penetration depths in the tests are 20–50 mm, the thickness of the individual layer is 0.2–0.5 mm. The model allows the material properties porosity f, permeability K and wet front capillary potential Ψ_{f} to vary from layer to layer. However within a single brick, variations in f, K and Ψ_{f} are likely to be correlated, perhaps strongly. (For example, in a generalised Kozeny-Carman material, $K \sim f^3/(1-f^2)$, and $\Psi_{\mathrm{f}} \sim K^{-1/2}$). Here, the best fit parameter values are those that minimise the sum of the squares of the residuals between data and model.

Fig 5 *Left* shows model fits which represent the *n*-decane imbibition data well. In this case, we constrain the fits by requiring that the local sorptivity estimated from the skin-up and skin-down tests should be the same at the same location. It is found that the decane sorptivity varies from about 0.35 mm/min$^{1/2}$ at the surface to about 1.60 mm/min$^{1/2}$ at a depth of 50 mm, close to the centre of the brick. (Results for these and other bricks are gathered in Table 3). The variation is roughly linear with distance from the surface, with some indication of change in slope at a depth of about 25 mm. Accompanying the variation in sorptivity there is also a variation in permeability. The analysis finds only the layer-to-layer variation in permeability ratio along the flow path, and in this case the permeability at the centre is about twice that at the surface skin. Most of the variation occurs in the surface 25 mm.

Fig 5 shows water imbibition through an Edinburgh bed face core. Again, the non-linearity in $i(t^{1/2})$ is striking, and the *n*-layer model also describes the data excellently. The water sorptivity varies from about 0.30 mm/min$^{1/2}$ at the surface to about 1.80 mm/min$^{1/2}$ at a depth of about 43 mm, roughly in the centre of the brick. The results from tests in which flow is from the interior outwards towards the surface (Fig 5A) and those in which the flow is from the skin inwards (Fig 5B) are in good agreement.

Table 3 Measured water sorptivity

Brick type	Face	Sorptivity $\mathrm{mm/min^{1/2}}$	
		Skin	*Interior*
Edinburgh	Stretcher	0.30	1.74
	Bed	0.30	1.80
Niddrie	Stretcher	0.56	0.51
	Bed	0.44	0.47
Prestongrange	Stretcher	1.90	2.17
	Bed	0.15	1.38
Wallyford	Stretcher	0.30	0.05
	Bed	0.15	0.08
Whitehill	Stretcher	1.50	1.65
	Bed	1.60	1.63

Generally similar behaviour is found in the stretcher face core of Edinburgh brick, as shown in Fig 6. Here the surface skin has water sorptivity $S = 0.30\,\mathrm{mm/min^{1/2}}$, rising to about $1.75\,\mathrm{mm/min^{1/2}}$ in the interior.

As Fig 7 shows, there is a marked skin effect in bed face cores of Prestongrange brick also. The water imbibition curves are similar to those of bed face Edinburgh core (Fig 5 *Right*). The best fit parameters indicate a low effective porosity, around 0.14–0.16, which we link tentatively to the presence of fissures which do not fill during imbibition. There is an abrupt increase in sorptivity about 25 mm below the surface and the surface sorptivity is about five times lower than that of the interior.

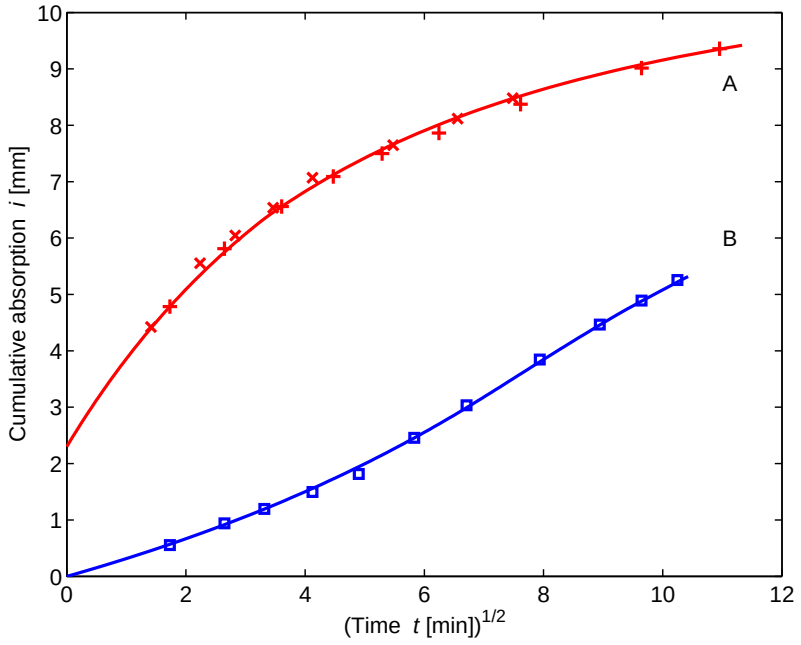

Fig. 6 Cumulative absorption i vs $t^{1/2}$ for imbibition of water into a stretcher face core of Edinburgh brick. Core length 60.8 mm × 24.4 mm diameter. Solid curves are fits to n-layer model with $n = 100$. *A*: Skin-up, flow towards the surface skin (repeat tests, +, ×); *B*: Skin-down, flow towards the interior.

5.2 Origins of surface skin

The data of Table 3 show that in the Edinburgh and Prestongrange bricks the sorptivity of the skin (with a thickness of roughly 20–25 mm) is much lower than that of the interior. From n-decane imbibition data on Edinburgh brick we also find from n-layer analysis that the skin has a markedly reduced permeability and a slightly reduced porosity. Measurements of tensile strength (I M Griffin, unpublished results) give

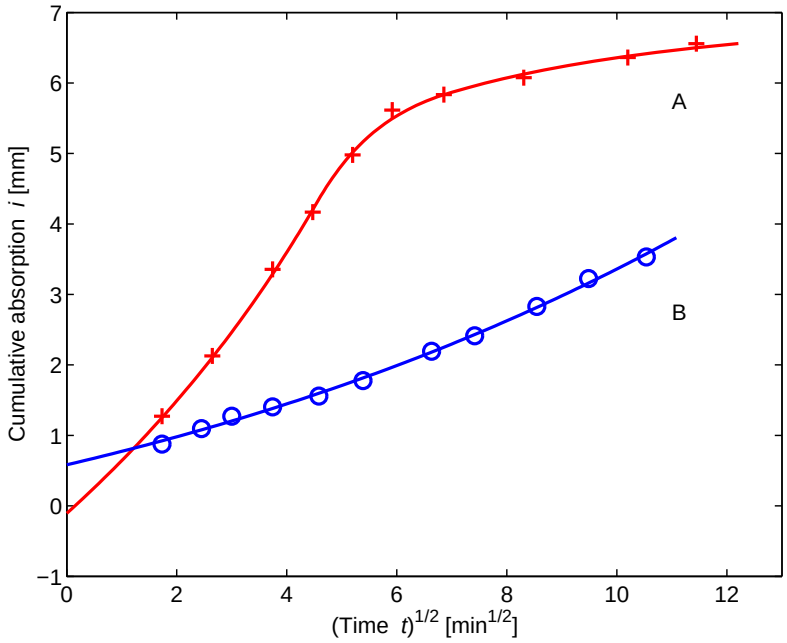

Fig. 7 Cumulative absorption i vs $t^{1/2}$ for imbibition of water into a bed face core of Prestongrange brick. Core length 59.0 mm × 24.1 mm diameter. Solid curves are fits to n-layer model with $n = 100$. *A*: Skin up, flow towards the surface skin; *B*: Skin down, flow towards the interior.

slightly higher values in samples taken from the the surface than in interior samples. Petrographic thin sections indicate that pores are preferentially aligned and elongated parallel to the surface. MIP measurements on the outer skin of the Prestongrange brick show a total volume fraction porosity of about 0.21, compared with 0.27 in the interior and the pore size distribution of the skin is coarser than that of the interior. These observations suggest that the reduction in sorptivity in the skin can be attributed

primarily to modification of microstructure during manufacture. The formation of a compact, low sorptivity surface layer during the firing process has been described previously [19]. This layer is visible in both the hand specimen and the thin section, and is most evident along the upper bed face of the brick, which presumably undergoes the greatest compaction inside the mould (Fig. 4). The main effect is probably to decrease the permeability by some degree of alignment of pores transverse to the capillary flow direction. This produces an increase in tortuosity, even if there is no change in pore size distribution.

One Edinburgh brick sample showed a high calcite content (Table 1), we therefore considered the possibility that the skin effect was caused by deposition of secondary calcite from cement/lime mortars. However treatment of a core with hydrochloric acid did not alter water absorption through the surface layer.

A well differentiated surface skin was not found in the other brick types, so it is clearly not an intrinsic feature of pressed colliery shale bricks.

5.3 Influence of wettability

It is known [10,19,25,26] that in modern production bricks the sorptivity measured with different liquids scales as the quantity $(\sigma/\eta)^{1/2}$, where σ is the surface tension and η the viscosity of the test liquid. This is true for organic liquids and for water, and shows that imbibition is a well behaved capillary process in which the pore surface is completely wetted. For other materials, notably building limestones [27,10], the behaviour of water is sometimes anomalous and the sorptivity does not scale as $(\sigma/\eta)^{1/2}$. For limestones, this is interpreted as evidence of partial wetting arising from a hydrophobic pore surface.

There is strong evidence of reduced wettability to water in most of these shale bricks, probably due to the notable content of residual organic material. For materials with non-uniform transport properties we can demonstrate partial wetting in two ways (see Fig 8). First, it is possible to compare water and *n*-decane imbibition data directly. The time $t(i)$ to reach a cumulative absorption i for a series of different liquids scales as σ/η for complete wetting. Deviations from this scaling indicate partial wetting. The wetting index β [10] usefully shows this. We define $\beta = t_{\rm d}\sigma_{\rm d}\eta_{\rm w}/(t_{\rm w}\sigma_{\rm w}\eta_{\rm d})$ so that β is the gradient of the line plotted in Fig 8 *Left*. When $\beta = 1$ we have complete wetting by water (no finite contact angle effects); when $\beta < 1$ the water wetting is partial (finite contact angle). The experimental data lie close to $\beta = 0.2$. In Fig 8 *Left*, we show Edinburgh core data presented in this way. The scaling deviation is striking, with $\beta \leq 0.2$ for water (corresponding to a dynamic contact angle of $\geq 70^\circ$).

The hydrophobicity of the material towards water is also clear from the ratio of the local sorptivities measured with the two liquids. From the $(\sigma/\eta)^{1/2}$ scaling we expect that at 21 °C , the ratio of water and *n*-decane sorptivities $S_{\rm w}/S_{\rm d}$ for complete wetting is 1.70. However for Edinburgh brick, $S_{\rm w}/S_{\rm d}$ is roughly 0.86 at the surface falling to around 0.69 at a depth of 27 mm, as shown for the skin-down tests in Fig 8 *Right*. Again, the data indicate a value of β close to 0.2, with a suggestion that β decreases slightly going from the surface to the interior, therefore the material is more hydrophobic in the interior than at the surface.

Wallyford brick is very unusual (Table 3), with its extremely low water sorptivity but normal *n*-decane sorptivity, see Fig 9. *n*-Decane imbibition scales as $t^{1/2}$, indicating uniformity of transport properties, and $S_{\rm d}$=0.75–0.79 mm min$^{1/2}$, similar to the decane sorptivity of Edinburgh brick. There is no significant difference between the sorptivity measured in skin up and skin down tests, confirming the absence of a skin effect in

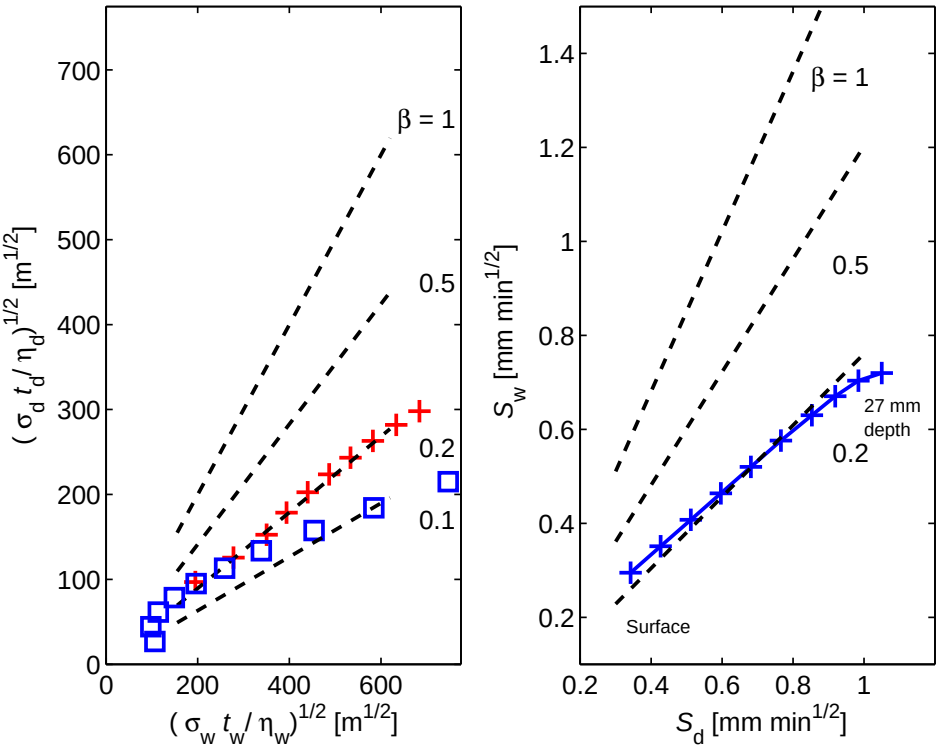

Fig. 8 Comparison of water and decane imbibition measured on a stretcher-face core of Edinburgh brick. *Left* Direct comparison of water and n-decane imbibition data (□ skin up test, + skin down test). The quantities t_w and t_d are the times required to reach equal cumulative absorptions i in the two liquids, obtained by interpolating $i(t)$ test data. Dotted lines show expected t_d and t_w for four values of the wetting index β. *Right* Cross plot of sorptivities, S_w, S_d, derived from n-layer model fits to data from skin down tests (flow from surface towards the interior). Data points show the increase in sorptivities over a total penetration distance of about 27 mm. Dotted lines show expected ratio S_w/S_d for three values of the wetting index β.

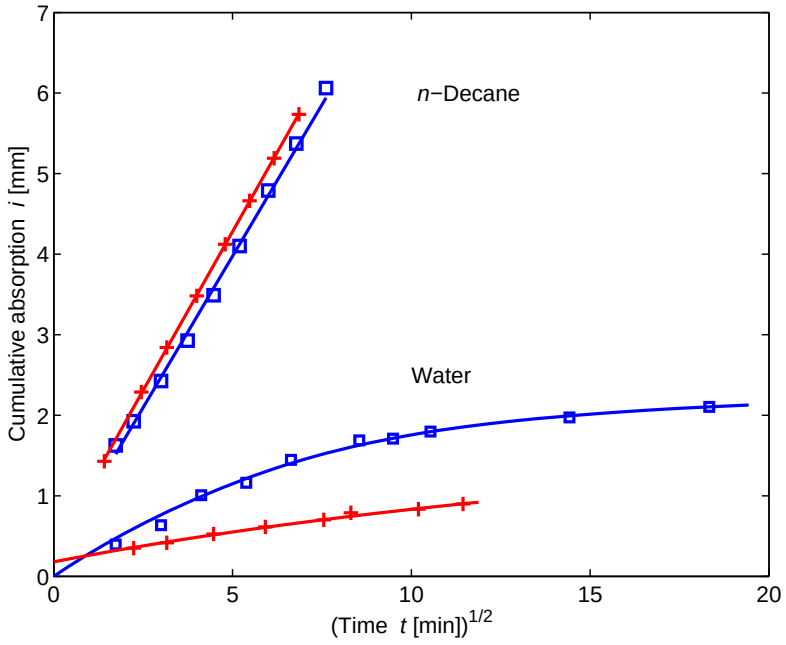

Fig. 9 Wallyford brick: Imbibition of n-decane and water compared. Cumulative absorption i vs $t^{1/2}$ into stretcher face core (length 59.0 mm × 24.1 mm diameter). Skin up data +, skin down data □. For water, solid curves are fits to n-layer model with $n = 100$, with S_{w} varying from 0.3 mm/min$^{1/2}$ at the surface to 0.05 mm/min$^{1/2}$ in the interior. For n-decane, solid lines are linear fits to $i = S_{\mathrm{d}}t^{1/2} + B$ (constant sorptivity), with $S_{\mathrm{d}} = 0.79$ mm/min$^{1/2}$ (skin up), and 0.75 mm/min$^{1/2}$ (skin down).

n-decane imbibition. In water imbibition, we see a weak skin effect, with the surface sorptivity slightly higher than the interior sorptivity. The water sorptivity is so low that β is close to zero. There is an indication that the hydrophobicity is slightly lower in the surface layer than in the interior and we link this unusual behaviour with the

exceptionally high interior organic carbon content of Wallyford brick (Table 1). The extremely hydrophobic character of the material we examined is seen dramatically in a simple test in which a droplet of liquid is placed on the surface of the core. A droplet of decane is absorbed within a few seconds while a droplet of water remains on the surface for many minutes.

5.4 Variations between cores drilled through the bed face and the stretcher face

It is known that some directionality occurs in the properties of fired clay ceramics, but this anisotropy has not been extensively or systematically investigated. It has been reported that the sorptivities measured on bed and stretcher faces of extruded production bricks are not the same [19, 28]. The only published information on pressed bricks that we have found is from Ince *et al.* [29] who describe sorptivity normal to the bed face of one British facing brick, measured on 25–30 mm slices varies along the bed face.

Generally, we do not see marked differences in sorptivity between stretcher face and bed face cores. The main exception occurs in Prestongrange brick where the stretcher face core has an extremely high sorptivity. In this material cracks run parallel to the bed face while the thin sections showed the presence of capillary pores up to 70 μm long and 10 μm wide, again aligned parallel to the bed face. Due to this, imbibing water can move rapidly along the core, producing a high apparent sorptivity.

The role of cracks in increasing sorptivity has implications for changes in the sorptivity over time, because cracks are likely to develop as a brick ages. Cracks may either enhance imbibition or act as a barrier to it, depending on size and orientation.

5.5 Variations in sorptivity between the types of bricks

We find remarkable differences in sorptivity between the brick types of this small set, although they have similar porosities and are products of a similar technology. These differences reflect the combined effects of composition (mineralogy), pore structure and wettability.

Although the sample set is small, we note some comparisons and patterns in the data. For example, it is likely that bricks with high mullite/quartz ratio (Prestongrange, Whitehill) were fired at higher temperature than those with low mullite/quartz ratio (Edinburgh, Niddrie). The higher-fired bricks are expected to have a coarser pore structure [30], and this is found to be reflected in the MIP measurements. The higher-fired bricks with coarser pore size distribution are expected to show slightly higher sorptivities, since at constant porosity the sorptivity scales as $\lambda^{1/2}$, where λ is a pore length-scale [10]. Consistent with this we note the high sorptivity of the Whitehill brick (high mullite/quartz ratio), and the low sorptivity of Niddrie brick (low mullite/quartz ratio). However our sample is small, and in some cases effects of microstructure on sorptivity are masked by wettability effects.

6 Conclusions

- We have shown how capillary imbibition data exhibiting marked non-linearity in $i(t^{1/2})$ behaviour can be analysed using an n-layer model to give estimates of the local sorptivity and permeability.
- In some traditional Scottish colliery shale bricks, we find that the sorptivity decreases from the surface to the interior. This skin effect is attributed to modification of the microstructure in a surface layer produced by moulding during manufacture.

- The water sorptivity of some of these bricks is anomalous in not scaling as $(\sigma/\eta)^{1/2}$. This indicates that the sorptivity is reduced by the partial wettability of the pore surface. We associate this unusual hydrophobicity with the high residual organic carbon content of these shale bricks.
- In this small set of materials, we see some differences between bed-face and stretcher-face sorptivity, consistent with the few scattered results published elsewhere. Anisotropy in the transport and other engineering properties of fired-clay brick has received little attention in spite of its obvious importance in performance and design.
- The variation of sorptivity between the bricks is remarkable considering their similar porosities, mineralogy and production technology. This suggests that the water transport properties of brick deserve more detailed and comprehensive study in the future, particularly in relation to anisotropy and wettability.

Acknowledgements This work was undertaken as part of a PhD project (IMG) funded by the UK AHRC and EPSRC through the Science and Heritage programme.

References

1. Lawson EM, Nixon PJ (1978) A survey of the locations, disposal and prospective uses of the major industrial by-products and waste materials in Scotland. Current Paper 50/78, Building Research Eastablishment, Garston
2. Lawson EM, Nixon PJ (1979) Prospective uses of Scotland's by-products. Ceram Ind J 88:21–23
3. Gutt W, Nixon PJ (1979) Use of waste materials in the construction industry. Mat Struct 12: 255–306
4. Douglas GJ, Oglethorpe MK (1993) Brick, tile and fireclay industries in Scotland, Royal Commission on the Ancient and Historical Monuments of Scotland, Edinburgh
5. British Geological Survey (2005) Brick clay. Mineral Planning Factsheet, BGS

6. Hall C (1996) Clay brick. In: Civil engineering materials, Eds. Jackson N, Dhir RK, 5th edn., Palgrave, Basingstoke and New York

7. Douglas GJ, Hume JR, Moir L, Oglethorpe MK (1985) A survey of Scottish brickmarks, Scottish Industrial Archaeology Survey, University of Strathclyde

8. Haibin, Liu, Zhenling, Liu (2010) Recycling utilization patterns of coal mining waste in China. Resources, Conservation and Recyling 54:1331–1340

9. Hyun J-Y, Jeong S-B, Chae Y-B, Kim B-S (2006) Development of fired clay bricks by coal-preparation refuse. J Ceram Soc Japan 114:404–407

10. Hall C, Hoff WD (2012) Water transport in brick, stone and concrete, 2nd edn., Taylor and Francis, London and New York

11. Hall C, Hoff WD (2007) Rising damp: capillary rise dynamics in walls. Proc Roy Soc A 463:1871–1884

12. Hall C, Hamilton A, Hoff WD, Viles HA, Eklund JE (2011) Moisture dynamics of walls: Response to microenvironment and climate change. Proc Roy Soc A, 467:194–211

13. Derluyn H, Janssen H, Carmeliet J (2011) Influence of the nature of interfaces on the capillary transport in layered materials. Constr Build Mater 25:3685–3693

14. Blocken B, Carmeliet J (2012) A simplified numerical model for rainwater runoff on building facades: Possibilities and limitations. Build Environ 53:59–73

15. Air Ministry (1997) The Royal Air Force builds for war: A history of design and construction in the RAF, 1935–1945, Stationery Office, London

16. Francis P (1996) British military airfield architecture. Patrick Stephens, Sparkford

17. http://www.penmorfa.com/bricks/scotland2.html, accessed 19/07/12

18. Aligizaki KK (2006) Pore structure of cement-based materials, Taylor and Francis, London and New York

19. Gummerson RJ, Hall C, Hoff WD (1980) Water movement in porous building materials – II. Hydraulic suction and sorptivity of brick and other masonry materials. Build Environ 15:101–108

20. Nicholson PS, Ross WA (1970) Kinetics of oxidation of natural organic material in clays. J Amer Ceram Soc 53:154–158

21. Dunham AC (1992) Developments in industrial mineralogy: I. The mineralogy of brickmaking. Proc Yorkshire Geol Soc 49:95–104

22. Dunham AC, McKnight AS, Warren I (2001) Mineral assemblages formed in Oxford Clay fired under different time-temperature conditions with reference to brick manufacture. Proc Yorkshire Geol Soc 53:221–230

23. Hall C, Hoff WD and Prout W (1992) Sorptivity-porosity relations in clay brick ceramic. Am Ceram Soc Bull 71:1112–1116

24. Hall C (2006) Anomalous diffusion in unsaturated flow–fact or fiction? Cem Concr Res 37:378–385

25. Beltrán V, Escardino A, Feliu C, Rodrigo MD (1988) Liquid suction by porous ceramic materials. Brit Ceram Trans J 87:64–69

26. Beltrán V, Barba A, Jarque JC, Escardino A (1991) Liquid suction by porous ceramic materials: 3 – Influence of the nature of the composition and the preparation method of the pressing powder. Brit Ceram Trans J 90:77–80

27. Ioannou I, Hoff WD, Hall C (2004) On the role of organic adlayers in the anomalous water sorptivity of Lépine limestone. J Colloid Interface Sci 279:228–234

28. Krakowiak KJ, Lourenço PB, Ulm F-J (2011) Multitechnique investigation of extruded clay brick microstructure. J Am Ceram Soc 94:3012–3022

29. Ince C, Carter MA, Wilson MA, El-Turki A, Ball RJ, Allen GC, Collier NC (2010) Analysis of the abstraction of water from freshly mixed jointing mortars in masonry construction. Mater Struct 43:985–992

30. Cultrone G, Sebastián E, Elert K, de la Torre MJ, Cazalla O, Rodriguez-Navarro C (2004) Influence of mineralogy and firing temperature on the porosity of bricks. J Eur Ceram Soc 24:547–564

31. Hall C, Green K, Hoff WD, Wilson MA (1996) A sharp wet front analysis of capillary absorption into n-layer composite. J Phys D: Appl Phys 29:2947–2950